A Flexible Wearable Patch for Biomedical Sensing Applications

Dilruba Alam*, Tasnim Zaman Adry*, Kedzie Kratzer*, Amelia Truong*, Sazia Eliza*, and Mohammad Rafiqul Haider*
*Department of Electrical Engineering and Computer Science
University of Missouri, Columbia, MO, USA
Email: {dilruba.alam, tzfft, kakypm, ajt9zn, seliza, mhaider}@missouri.edu

***Abstract*—This paper addresses the urgent need for advanced health monitoring solutions tailored for next-generation smart screening and diagnostics. We propose a novel approach utilizing a lightweight, low-power, and cost-effective wearable patch, designed to overcome the limitations of traditional bulky sensing units. Our innovative design features a flexible electrode grid with minimized wiring, integrated sensor readout electronics, and inkjet-printed spiral coils, enabling efficient wireless charging. The electrode grid manifests an array of sensing pads encircled by a reference terminal, which can be selectively excited by a constant potential. The electrode grid measures the impedance between the sensing pad and the reference ring and generates a current proportional to the sensing material. The sensor current is then passed through a multichannel inverting amplifier to generate the output signal. The printed spiral coils work in resonant mode to couple power from an external source to the wearable patch to power up the electronics. This work aims to provide a practical and affordable solution for real-world health monitoring applications, paving the way for widespread deployment in diverse settings.**

***Index Terms*—electrode grid, printed inductive coils, wearable sensor.**

I. Introduction

In recent years, wearable biomedical technologies have experienced exponential growth, driven by the growing demand for real-time, continuous health monitoring, and personalized healthcare solutions. According to recent market research, the global wearable medical devices market is expected to reach USD 174.48 billion by 2030, expanding at a compound annual growth rate (CAGR) of 25.2% from 2023 to 2030 [1]. Wearable sensors are being increasingly deployed for monitoring physiological parameters such as heart rate, hydration level, glucose concentration, and skin temperature.

Despite this growth, traditional rigid sensors present challenges such as discomfort during prolonged use, mechanical mismatch with skin, and susceptibility to motion artifacts [2]. Flexible and stretchable electronics offer promising alternatives that can conform to body surfaces, providing better mechanical compatibility and user comfort [3].

In addition to mechanical compliance, efficient electronics design is crucial for wearable health systems. Ultra-low-power signal processing circuits are necessary to handle small biosensor currents while minimizing energy consumption, especially in continuous monitoring applications [4], [5]. Inkjet printing offers low-cost, high-quality, and high-throughput advantages for large-scale fabrication of flexible and wearable electronics, benefiting applications like portable health monitoring and human-machine interaction [6]–[9]. Integrating electronics, like amplifiers and interconnects, further enhances device adaptability without compromising performance [10], [11].

Moreover, traditional battery-powered wearable systems often suffer from limited operational lifetimes, frequent recharging requirements, and bulky designs, limiting their suitability for continuous health monitoring [12]. To overcome these limitations, researchers have increasingly turned to wireless power transfer (WPT) technologies, particularly those utilizing resonant inductive coupling, as a promising solution [13].

Recent advances in flexible electronics have further enabled the seamless integration of wireless power receivers directly onto soft substrates. In particular, inkjet-printed spiral coils tuned to resonant frequencies have demonstrated efficient wireless charging performance while preserving the flexibility and conformability essential for wearable applications [14], [15]. These printed coils allow the patch to maintain minimal thickness and mechanical adaptability without sacrificing electrical performance.

In this work, a flexible wearable patch that integrates a printed electrode grid for impedance-based biosensing, wireless energy harvesting coils, and signal readout circuitry, as demonstrated in Fig. 1. Equally important to system performance is the design of the electrode grid, which dictates the resolution of the detection, mechanical robustness, and signal fidelity. Traditional wired electrode designs often introduce bulk, reduce spatial resolution, and are prone to motion artifacts. To address these challenges, a field-referenced electrode structure—where a sensing pad is surrounded by a reference ring—can be employed to enhance localized impedance sensing and reduce crosstalk between adjacent electrodes [16]–[18]. This architectural approach focuses the electric field lines onto the sensing pads, improving sensitivity and selectivity even under dynamic conditions.

The organization of the rest of the paper is as follows. Section II discusses the overall device architecture and its working principle. Section III presents the design and fabrication process of the electrode grid and printed spiral coils, followed by experimental analysis and characterization in

This work was partially supported by National Science Foundation (NSF), USA award no. ECCS-2430440.

Section IV. Finally, Section V draws the conclusion and highlights future directions.

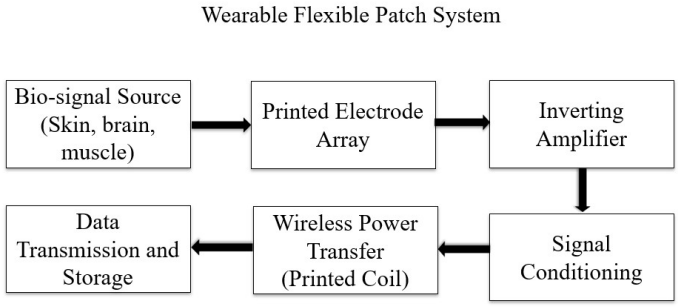

Fig. 1. Block diagram of the designed system.

II. System Overview

The proposed system manifests a flexible electrode grid for impedance monitoring, read-out electronics for multichannel sensor signal processing, and a printed spiral coil-based wireless powering of the read-out electronics. A short description of each of the functional blocks is provided as follows.

A. Electrode Grid

The electrode structure consists of a central sensing disc surrounded by a concentric reference ring, with a dielectric layer in between to provide electrical isolation, as shown in Fig. 2. By applying a reference voltage to the surrounding ring, the electric field originating from a biosignal source becomes focused toward the center-sensing electrode. The electrode grid forms the primary biosignal interface. The referenced field structure improves spatial resolution by concentrating the bioelectric field lines toward the sensing pad and protecting it from neighboring interference [16].

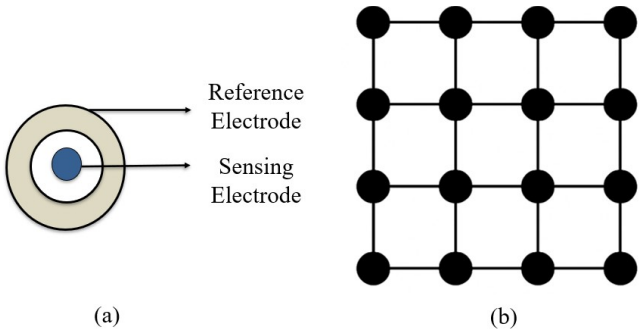

Fig. 2. (a) Cross-sectional view of a concentric electrode structure consisting of a central sensing electrode surrounded by a reference electrode, electrically isolated via a dielectric layer; (b) Topology of a 4×4 electrode array layout.

B. Sensor Readout Electronics

The sensor readout electronics are designed to capture and amplify weak bioelectric signals generated at each sensing electrode. It comprises a multichannel inverting amplifier. A multichannel inverting amplifier is a signal processing architecture used to amplify multiple weak input signals independently using inverting operational amplifiers (op-amps). This is especially useful for bioelectrical signal acquisition, where multiple electrodes capture voltages at different locations in the body.

Inverting Amplifier Principle

In an inverting amplifier, the input signal is fed through a resistor R_{in} to the inverting terminal of the op-amp, while the non-inverting terminal is connected to a common reference voltage (e.g., ground or mid-supply voltage).

The output voltage is given by:

$$V_{\text{out}} = -\left(\frac{R_f}{R_{\text{in}}}\right) V_{\text{in}} \tag{1}$$

where:

- V_{in} is the voltage from an individual electrode
- R_{in} is the input resistor
- R_f is the feedback resistor

C. Wireless Charging Link

Traditional wearable devices often depend on batteries or wired connections, which introduce limitations such as increased weight, frequent maintenance, and restricted user mobility. Wireless power transfer offers a more elegant solution by eliminating physical connectors while maintaining continuous operation [19]–[21].

Among wireless methods, resonant inductive coupling stands out for its ability to efficiently transmit power over small distances without direct contact. This approach pairs transmitter and receiver coils with carefully matched capacitors, forming a resonant LC network that maximizes energy transfer through synchronized magnetic field oscillations. The system operates on the basis of coupled-mode theory, where the Tx and Rx coils form a resonant circuit when:

$$\omega_0 = \frac{1}{\sqrt{L_s C_s}} = \frac{1}{\sqrt{L_d C_d}} \tag{2}$$

where L_s, C_s and L_d, C_d are the inductance/capacitance of the source coils (Tx) and the device coils (Rx), respectively, and ω_0 is the angular resonant frequency. The efficiency of the system is further enhanced by incorporating a passive repeater coil, which extends the effective charging range by improving magnetic flux coupling as shown in Fig. 3.

Unlike rigid battery-based solutions, this wireless link integrates seamlessly into flexible wearable designs, allowing for slim, unobtrusive form factors. The wearable patch integrates inkjet-printed spiral coils to enable efficient wireless charging, eliminating the need for rigid batteries. The coils are strategically placed below the electrode grid to maintain the slim profile of the patch.

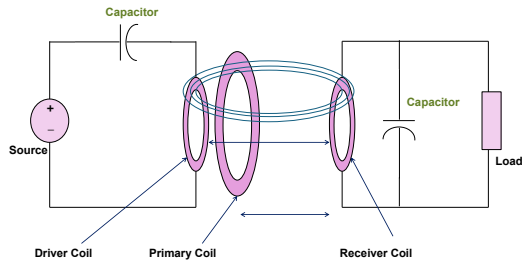

Fig. 3. Inductive Charging link with repeater coil which can extend the charging range.

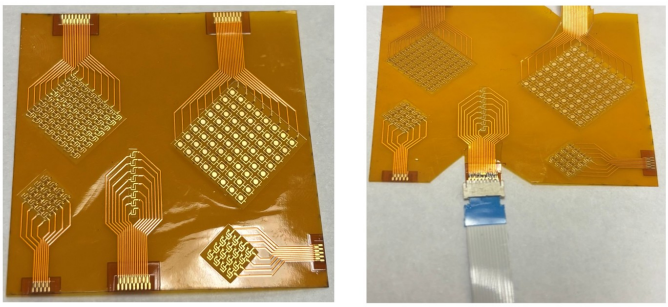

(a) (b)

Fig. 4. Electrode grid structure: (a) Printed impedance sensing network on flexible Kapton substrate. Various layouts with interleaved sensing and reference electrodes designed for impedance and bio-signal acquisition (b) Experimental test setup of the electrode grid using ribbon cable and connector for external interface.

III. Design and Fabrication

The electrode grid was designed using a PCB design software and fabricated on a flexible polyimide film.

The planar spiral coil was designed in CAD software and fabricated on a flexible PET film using silver nanoparticle-based ink with the Voltera V-One PCB printer. The coil design is shown in Fig. 5. The design, featuring 25 turns with a 0.5 mm trace width and 0.5 mm spacing, was optimized to function as an LC resonator for resonant inductive coupling.

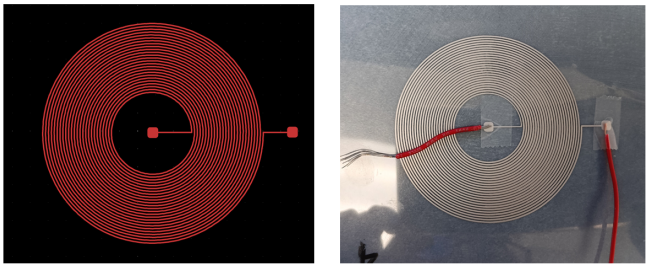

Fig. 5. (a) CAD design of the planar spiral coil showing geometry (b) Fabricated flexible coil with silver nanoparticle ink traces on polymer substrate.

IV. Experimental and Simulation Results

A. Characterization of the Electrode Grid

The electrode was characterized using a Source-Measure-Unit (SMU). A precise voltage (21.0 V) was applied across the device under test (DUT), while the resulting current and impedance were measured with high sensitivity (in the sub-microampere range). The DUT—a flexible printed electrode array on a polyimide substrate—is connected to the Source Meter via standard banana-to-alligator clip leads through a ribbon connector and electroode sensitivity with the force of contact was measured.

TABLE I
Measured Impedance Variations under Different Contact Conditions (Voltage Source: +21.0 V)

Contact Condition	Impedance (MΩ)	Measured Current (μA)
Firm contact	9–10	0.019–0.028
Medium contact	10–30	0.010–0.015
Light contact	50–200	0.010–0.050
No contact	250	0.001

B. Multichannel Inverting Amplifier Simulation

The resistance change of the sensor is processed through a multichannel inverting amplifier-based sensor readout system.

Fig. 6 shows the schematic of a multichannel inverting amplifier, where non-overlapping pulsed sources of 250 mV excitation signals are used to simulate the effect of different channels. Each channel represents different resistance values of the sensors centered around the nominal 250 MΩ. A 250 MΩ feedback resistor (R3) sets the gain, while a 2.5 V DC reference (V3) is applied to the non-inverting input. The circuit operates with a single supply (Vdd = +5 V and Vss = 0 V). The multichannel amplifier operates on a time-division multiplexing (TDM) scheme using non-overlapping excitation pulses. Although simultaneous readout is not achieved, this architecture enables channel-wise sequential measurement with minimal hardware complexity

The output voltage of the circuit can be expressed as:

$$V_{\text{out}} = V_3 - R_3 \left(\frac{V_2}{R_1} + \frac{V_{10}}{R_4} + \frac{V_{11}}{R_5} + \frac{V_{12}}{R_6} \right) \tag{3}$$

where R_3 is the feedback resistor, V_3 is the reference voltage, V_1, V_{10}, V_{11}, and V_{12} are the input voltages, and R_1, R_4, R_5, and R_6 are the respective input resistors. A transient simulation of the multichannel amplifier shown in Fig. 7 indicates different channel outputs corresponding to the individual channel gain with the respective channel selector signal.

C. Simulation of the Spiral Coil-Based Wireless Link

The fabricated spiral coils underwent comprehensive electrical characterization using a high-precision LCR meter capable of frequency sweeps from 10 Hz to 10 MHz. Through systematic frequency-domain analysis, we identified the optimal operating parameters—including series inductance (L_s),

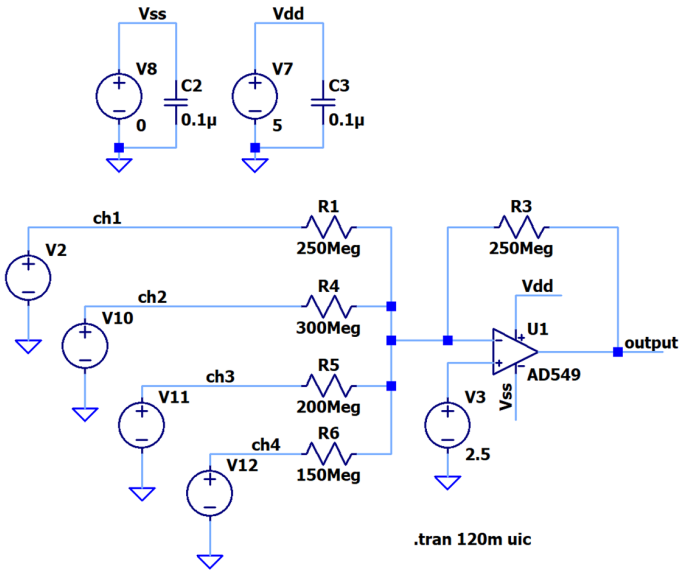

Fig. 6. Schematic of a multichannel inverting amplifier.

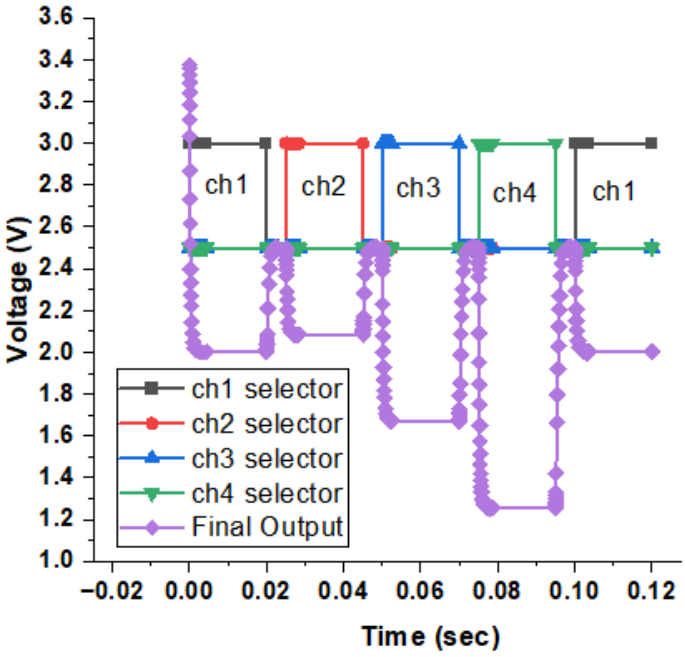

Fig. 7. Output response from the multichannel inverting amplifier.

series resistance (R_s), and quality factor (Q)—which are critical for efficient resonant power transfer. The printed coils demonstrated peak performance in the low-frequency range, exhibiting an inductance of 27 μH with a quality factor of 30 at 100 kHz frequency of operation.

These parameters informed the design of an LC resonant network, which was modeled and simulated using LTSpice circuit analysis software. The simulation results confirmed a stable DC output at the load side, validating the power transfer capability of the system. Fig. 8 presents both the complete

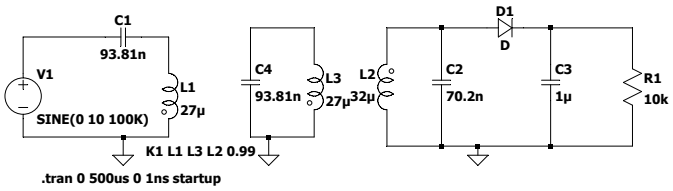

Fig. 8. Schematic of the inductive charging link.

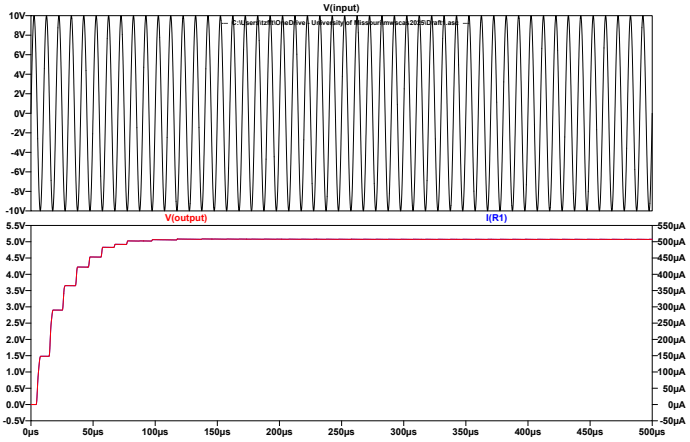

Fig. 9. Input signal from the voltage source and output signal taken from the load (R1).

circuit schematic and Fig. 9 presents the corresponding simulation waveforms, demonstrating the proper resonance at the target frequency. A 10V supply voltage applied to the primary side successfully delivers 5V to the load and the total power received is 2.5 mW, demonstrating the efficacy of the printed spiral coils as an efficient wireless charging link.

V. Conclusion

This work presented a flexible and integrated wearable sensing patch that combines a concentric electrode array, multichannel readout electronics, and inkjet-printed spiral coils for wireless power transfer. The system was designed for impedance-based biosignal acquisition, and preliminary electrical characterization confirmed the functionality of both the electrode interface and the amplifier stages. The electrode data suggest that moderate contact provides an optimal balance between user comfort and reliable electrical performance. However, this study is currently limited to benchtop electrical validation. Future work will focus on acquiring and analyzing real biosignals (e.g., ECG or EMG) using the electrode array. Additionally, integration with a microcontroller and wireless data transmission module will be explored to complete the system for real-time monitoring.

Acknowledgment

In this work, Ms. Kadzie Kratzer and Ms. Amelia Truong worked as undergraduate research assistants. Ms. Dilruba Alam, Ms. Tasnim Zaman Adry, Ms. Kedzie Kratzer, and Ms. Amelia Truong has an equal contribution to the paper.

REFERENCES

[1] S. Patel, H. Park, P. Bonato, L. Chan, and M. Rodgers, "A review of wearable sensors and systems with application in rehabilitation," *Journal of NeuroEngineering and Rehabilitation*, vol. 9, no. 1, p. 21, 2012.

[2] J. Heikenfeld, A. Jajack, J. Rogers, et al., "Wearable sensors: Modalities, challenges, and prospects," *Lab on a Chip*, vol. 18, no. 2, pp. 217–248, 2018.

[3] A. J. Bandodkar, I. Jeerapan, and J. Wang, "Wearable chemical sensors: Present challenges and future prospects," *ACS Sensors*, vol. 4, no. 2, pp. 295–304, 2019.

[4] M. Zhang, M. R. Haider, M. A. Huque, M. A. Adeeb, S. Rahman, and S. K. Islam, "A Low Power Sensor Signal Processing Circuit for Implantable Biosensor Applications," *Smart Materials and Structures*, vol. 16, no. 2, pp. 525–530, 2007.

[5] R. R. Harrison and C. Charles, "A low-power low-noise CMOS amplifier for neural recording applications," *IEEE Journal of Solid-State Circuits*, vol. 38, no. 6, pp. 958–965, 2003.

[6] K. Yan, J. Li, L. Pan, and Y. Shi, "Inkjet printing for flexible and wearable electronics," *APL Materials*, vol. 8, no. 12, p. 120705, 2020. https://doi.org/10.1063/5.0031669.

[7] A. Kamyshny and S. Magdassi, "Conductive nanomaterials for printed electronics," *Small*, vol. 10, no. 17, pp. 3515–3535, 2014.

[8] T. Carey, S. Cacovich, G. Divitini, J. Ren, A. Mansouri, J. M. Kim, et al., "Fully inkjet-printed two-dimensional material field-effect heterojunctions for wearable and textile electronics," *Nature Communications*, vol. 8, no. 1, p. 1202, 2017.

[9] T. Z. Adry, S. Akter, S. Eliza, S. D. Gardner, and M. R. Haider, "An inkjet-printed flexible memristor device for echo state networks," in *Proc. 2024 IEEE Computer Society Annu. Symp. VLSI (ISVLSI)*, Jul. 2024, pp. 740–744.

[10] H. Sirringhaus, "Inkjet Printing of Functional Materials," *Materials Today*, vol. 9, no. 4, pp. 28–35, 2006.

[11] J. Kim, M. Lee, H. J. Shim, R. Ghaffari, H. R. Cho, D. Son, et al., "Stretchable silicon nanoribbon electronics for skin prosthesis," *Nature Communications*, vol. 5, no. 1, p. 5747, 2014.

[12] J.-W. Jeong, W.-H. Yeo, A. Akhtar, et al., "Materials and Optimized Designs for Human-Machine Interfaces via Epidermal Electronics," *Advanced Materials*, vol. 25, no. 47, pp. 6839–6846, 2013.

[13] S. Kim, J. Kim, and J. Kim, "Wireless Power Transfer for Wearable Devices: From Flexible Coils to Integrated Systems," *Micromachines*, vol. 12, no. 6, p. 654, 2021.

[14] Y. Khan, A. E. Ostfeld, C. M. Lochner, A. Pierre, and A. C. Arias, "Monitoring of Vital Signs with Flexible and Wearable Medical Devices," *Advanced Materials*, vol. 28, no. 22, pp. 4373–4395, 2016.

[15] Y. Li, N. Grabham, R. Torah, J. Tudor, and S. Beeby, "Textile-based flexible coils for wireless inductive power transmission," *Applied Sciences*, vol. 8, no. 6, p. 912, 2018.

[16] S. A. Eliza, A. L. Paige, and M. R. Haider, "A Field-Referenced Surface Electrode for Biosignal Detection," *8th International Conference on Electrical and Computer Engineering (ICECE)*, pp. 73–76, 2014.

[17] Y. M. Chi, Y. T. Wang, Y. Wang, C. Maier, T. P. Jung, and G. Cauwenberghs, "Dry and noncontact EEG sensors for mobile brain–computer interfaces," *IEEE Transactions on Neural Systems and Rehabilitation Engineering*, vol. 20, no. 2, pp. 228–235, 2011.

[18] J. Xu, S. Mitra, C. Van Hoof, R. F. Yazicioglu, and K. A. Makinwa, "Active electrodes for wearable EEG acquisition: Review and electronics design methodology," *IEEE Reviews in Biomedical Engineering*, vol. 10, pp. 187–198, 2017.

[19] M. R. Haider, S. K. Islam, S. Mostafa, M. Zhang, and T. Oh, "Low-power low-voltage current read-out circuit for inductively-powered implant system," *IEEE Transactions on Biomedical Circuits and Systems*, vol. 4, no. 4, pp. 205-213, Aug. 2010.

[20] U. M. Jow and M. Ghovanloo, "Design and optimization of printed spiral coils for efficient transcutaneous inductive power transmission," *IEEE Transactions on Biomedical Circuits and Systems*, vol. 1, no. 3, pp. 193–202, 2007.

[21] M. A. Adeeb, A. B. Islam, M. R. Haider, F. S. Tulip, M. N. Ericson, and S. K. Islam, "An inductive link based wireless power transfer system for biomedical applications," *Hindawi Active and Passive Electronic Components*, Article ID: 879294, 11 pages, DOI: 10.1155/2012/879294.